



ELSEVIER

Available online at www.sciencedirect.com

SCIENCE @ DIRECT®

Physics Letters A 323 (2004) 267–277

PHYSICS LETTERS A

www.elsevier.com/locate/pla

Dynamical analysis of a helium glow discharge. I A model

Arnaud Bultel^{a,*}, Christophe Letellier^a, Anne Bourdon^b

^a CORIA, UMR CNRS 6614, Université de Rouen, Site universitaire du Madrillet, Avenue de l'Université, 76801 Saint-Etienne du Rouvray cedex, France

^b Laboratoire EM2C, UPR CNRS 288, Ecole Centrale de Paris, 1, grande voie des Vignes, 92295 Châtenay-Malabry cedex, France

Received 20 April 2003; received in revised form 6 January 2004; accepted 31 January 2004

Communicated by F. Porcelli

Abstract

In this Letter, we investigate a model elaborated by Wilke et al. to explain various regimes observed in a helium glow discharge [Phys. Lett. A 136 (1989) 114] for which the underlying dynamics can be chaotic, quasi-periodic, etc. We found that this model does not obey all the required physical principles. A new one is therefore proposed. It is mainly based on separated balance equations for charged species resulting from the propagation of ionization waves.

© 2004 Elsevier B.V. All rights reserved.

PACS: 52.80.-s; 52.35.Mw; 82.33.Xj

Keywords: Chemical kinetics; Chaotic regimes; Ionization waves

1. Introduction

The positive column of a dc or ac glow discharge in metallic vapors, noble or molecular gases is almost always crossed by moving striations leading to quick oscillations of the light intensity collected at a given location [2]. Rayment and Twiddy have experimentally established that these waves are accompanied by oscillations of the electron energy distribution function (*eedf* in the following) [3]. If the discharge voltage is disturbed periodically by an ac voltage with a low modulation depth m , the frequency of the striations locks on that of the periodic excitation following a linear regime. By increasing m , a frequency spectrum of

the collected light intensity containing subharmonics and broadband noise is observed: for particular values of the control parameters, these striations may become chaotic [4].

In order to identify the main processes responsible for the behaviors observed in the case of helium (see the experimental device in Fig. 1) for the conditions summarized in Table 1 and to analyze the influence of chemistry, Wilke et al. [1] developed a non-linear chemical model based on the balance equation for electrons and excited atoms. After introducing their set of equations that do not satisfy all the physical principles, a new set of equations is discussed. These equations involve new rate coefficients from up-dated data for the elementary processes. Moreover, we discuss thoroughly the propagation of ionization waves and their influence upon these equations in order to complete the model.

* Corresponding author.

E-mail address: arnaud.bultel@coria.fr (A. Bultel).

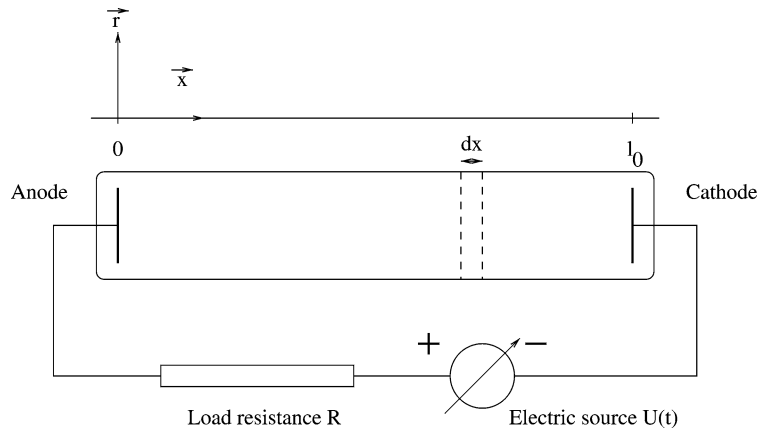


Fig. 1. Schematic experimental device used by Wilke et al. where the voltage delivered by the electric source is $U(t) = U_0(1 + m \cos \Omega t)$.

Table 1
Experimental conditions for the model by Wilke et al. (see Fig. 1 for the device)

Parameter	Notation	Value
Discharge length	l_0	41 cm
Radius	r_0	1 cm
Temperature	T_0	300 K
Pressure	p_0	1.8 Torr
Current	i_0	1–5 mA

The subsequent part of this Letter is organized as follows. Section 2 introduces the model by Wilke and his co-workers. In Section 3 an improved set of equations is proposed for a better description of the physical processes. Section 4 gives a conclusion.

2. The model by Wilke et al.

The balance equation for the electrons and the excited atoms of helium is written under the form:

$$\frac{\partial n_j}{\partial t} + \frac{\partial I_j}{\partial x} + \frac{n_j}{\tau_j} - P_j = 0, \quad (1)$$

where n is the density of the particles, I their flux density and τ their lifetime due to the diffusion to the wall of the cylinder containing the plasma and the destruction by chemical reactions. $j = a$ for the excited atoms and $j = e$ for electrons. P_j is their production rate.

In the case of electrons, the electroneutrality leads to a uniform electric field in the positive column so that

$\partial I_j / \partial x$ is reduced to the contribution of the diffusion. Moreover, this leads to the ambipolar approach. The orders of magnitude for the mobilities of ions and electrons as well as their diffusion coefficients allow the ambipolar diffusion coefficient to be written under the following form:

$$D_{am} = \frac{b_p}{b_e} D_e, \quad (2)$$

where b_e , b_p and D_e are the mobilities for the electrons, the ions and the diffusion coefficient of the electrons, respectively. According to Wilke and co-workers [1], Eq. (1) becomes:

$$\frac{\partial n_e}{\partial t} + \frac{b_p}{b_e} D_e \frac{\partial^2 n_e}{\partial x^2} + \frac{n_e}{\tau_e} - P_e = 0. \quad (3)$$

Hence, the diffusion flux density is:

$$I_e = + \frac{b_p}{b_e} D_e \frac{\partial n_e}{\partial x} \quad (4)$$

for which b_e , b_p and D_e are uniform. This form cannot be correct since it suggests a drift velocity oriented towards the highest concentrations of electrons when there is no external source such as an electric field. This is in conflict with the second law of thermodynamics. Such a contradiction will have deep consequences on the dynamics. In particular, the chaotic behaviors generated by this model and experimentally observed will not be recovered with a corrected diffusion flux density. This will be detailed later.

Table 2

Rate coefficients in $\text{m}^3 \text{s}^{-1}$ used by Wilke et al. and us. The reduced electric field is expressed in Td ($1 \text{ Td} = 10^{-21} \text{ V m}^2$)

Rate coeff.	Value used by Wilke et al. [1]	Our value
$z_{0\infty}$	$4.08 \times 10^{-28} (E/n)^{7.3}$	$1.8 \times 10^{-25} (E/n)^{5.6}$
$z_{a\infty}$	$2.70 \times 10^{-14} (E/n)^{0.65}$	\Leftarrow the same
z_a	1.1×10^{-15}	see Table 3
z_{me}	$3 \times 10^{-13} + 5.15 \times 10^{-16} (E/n)$	$2.4 \times 10^{-14} (E/n)^{0.44}$
z_{0a}	$7.01 \times 10^{-23} (E/n)^{4.5}$	$8.7 \times 10^{-21} (E/n)^{2.8}$

The usual assumption about the radial diffusion is to consider only the fundamental mode corresponding to the most important characteristic time. Moreover, the bulk recombination is neglected: τ_j is therefore proportional to r_0^2/D_j .

The chemical reactions taken into account result from the simplified energetic diagram. Considering the ground state, the excited levels and the fundamental level of the ions, the electrons are produced by direct ionization of the atoms under electron impact (the rate coefficient is $z_{0\infty}$), stepwise ionization of the excited atoms (with the rate coefficient $z_{a\infty}$) and Penning ionization (the rate coefficient is z_a). The rate coefficients used by Wilke et al. are reported in Table 2. The reduced electric field E/n is expressed in Td: we preferred this unit since it is the convenient one for electric discharge problems.

Since the diffusion of the excited atoms may be neglected along the discharge axis, Eq. (1) applied to them is rewritten under the form:

$$\frac{\partial n_a}{\partial t} + \frac{n_a}{\tau_a} - P_a = 0. \quad (5)$$

The loss term n_a/τ_a takes into account the radial diffusion to the wall (where once again only the fundamental mode is considered), the Penning ionization, the destruction of the metastable atoms by electron impact (rate coefficient z_{me}) and the stepwise ionization of the other excited atoms. Finally, the production rate P_a for excited atoms results from the total excitation under electron impact (rate coefficient z_{0a}).

According to Wilke et al., Eq. (3) becomes:

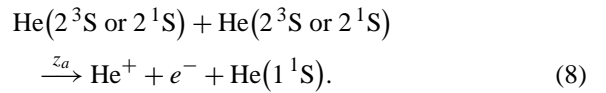
$$\frac{\partial n_e}{\partial t} + \frac{b_p}{b_e} D_e \frac{\partial^2 n_e}{\partial x^2} + \frac{\lambda_1^2 D_{am} n_e}{r_0^2} - n n_e z_{0\infty} - 1.45 n_a n_e z_{a\infty} - 1.45 n n_a z_a = 0, \quad (6)$$

where n is the total density of the plasma, and Eq. (5) takes the form:

$$\frac{\partial n_a}{\partial t} + \frac{\lambda_1^2 D_m n_a}{r_0^2} + 1.45 n_a^2 z_a + 1.45 n_e n_a z_{me} + 1.45 n_e n_a z_{a\infty} - n n_e z_{0a} = 0. \quad (7)$$

The value 1.45 is due to the radial average of the quantities as explained in the recent publication by Koch et al. [5] and λ_1 is the first root of the zeroth order Bessel function.

Eqs. (6) and (7) cannot be correct because the Penning ionization is produced by the collision between two metastable atoms according to the process:



Thus, the term $1.45 n n_a z_a$ in Eq. (6) should be $1.45 n_a^2 z_a$ instead and the term $1.45 n_a^2 z_a$ in Eq. (7) has to be multiplied by a factor 2.

Assuming stationary wave propagation for the electrons, Wilke et al. assumed that D'Alembert's equation

$$\frac{\partial^2 n_e}{\partial t^2} = v^2 \frac{\partial^2 n_e}{\partial x^2}, \quad (9)$$

where v is the group velocity is fulfilled. Unfortunately, this equation is not appropriate in this context because the chaotic behavior of the local light flux may have two simultaneous physical origins for preventing a steady wave. Either stationary electron density profile is accelerated or broken during its propagation along the discharge axis, or this profile is excited or damped during its propagation with constant velocity. In both cases, D'Alembert's equation is incomplete and an additional term has to be inserted accounting for the necessary unsteady wave propagation. Moreover, D'Alembert's equation cannot be external to the balance equations but must result from them.

The dynamical variables are normalized according to:

$$X = 10^6 \frac{n_e}{n}, \quad Y = 10^6 \frac{n_a}{n}, \quad \tau = 10^4 t. \quad (10)$$

Using these variables and Eqs. (6) and (7), Wilke et al. obtained the set of ordinary differential equations (o.d.e. system) as follows:

$$\frac{dX}{d\tau} = Z, \quad (11a)$$

$$\frac{dZ}{d\tau} = -C_1 \left\{ z - \left[\left(10^{-5} \left(\frac{E}{p_0} \right)^{7.3} - 7.44 \left(\frac{E}{p_0} \right)^{0.3} \right) X + 0.52 \left(\frac{E}{p_0} \right)^{0.65} XY + 0.01 Y^2 \right] \right\}, \quad (11b)$$

$$\frac{dY}{d\tau} = -0.15Y + 0.072 \left(\frac{E}{p_0} \right)^{4.5} X - 0.01Y^2 - \left[2.6 + 0.15 \left(\frac{E}{p_0} \right) + 0.52 \left(\frac{E}{p_0} \right)^{0.65} \right] XY. \quad (11c)$$

Eq. (11b) shows that the term $1.45n_a^2 z_a$ must have been used in Eq. (6). In this second equation,

$$C_1 = \frac{10^{-4} b_e v^2}{b_p D_e} \quad (12)$$

is constant. The reduced electric field is kept under the form E/p_0 for easier comparisons with the work by Wilke et al.

In fact, this set of equations cannot be obtained from Eqs. (6) and (7). Indeed, after some algebra, Eq. (11b) becomes instead:

$$\frac{dZ}{d\tau} = -C_1 \left\{ z - \left[\left(10^{-5} \left(\frac{E}{p_0} \right)^{7.3} - \frac{\lambda_1^2 D_{am}}{10^4 r_0^2} \right) X + 0.52 \left(\frac{E}{p_0} \right)^{0.65} XY + 0.01 Y^2 \right] \right\}. \quad (13)$$

In order to ensure identity between these equalities, the ambipolar diffusion coefficient has to be electric field dependent: C_1 is therefore a function of E/p_0 (cf. Eqs. (2) and (12)). This was not taken into account in Wilke's investigations since all the numerical simulations were done with $C_1 = 2$. Moreover, it is important to note that deducing Eq. (1) from the general

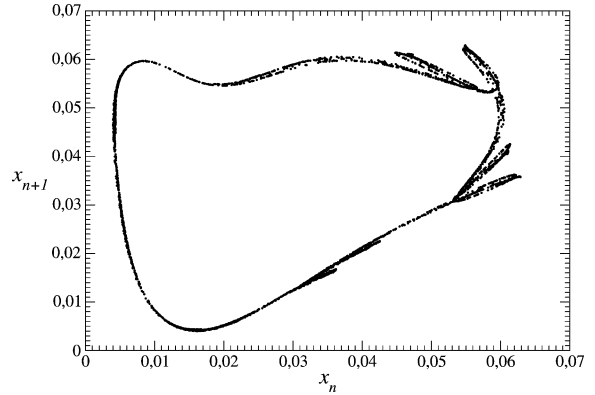


Fig. 2. Poincaré section computed from the set of equations proposed by Wilke et al. with parameters corresponding to Fig. 8c of their paper with the exception of C_2 here equal to 0.294.

balance equation (see Deloche et al. [6]) is equivalent to the assumption of an isotropic diffusion coefficient. In Eq. (6), $b_p D_e / b_e$ and D_{am} are consequently strictly identical. If we suppose a relationship between the latter and E/p_0 , then $b_p D_e / b_e$ presents the same characteristic.

Finally, the coupling of the chemistry of the plasma with the external current circuit allows E/p_0 to be expressed in terms of the external voltage:

$$\frac{E}{p_0} = C_2 \frac{1 + m \cos \Omega \tau}{X + 0.005}. \quad (14)$$

With the system proposed by Wilke and co-workers, we computed a Poincaré section (Fig. 2) with the parameters: $C_1 = 2$, $m = 0.5$, $C_2 = 0.25195$ and $\Omega = 2 \times 10^{-4} \pi f_a = 4$ where f_a is the frequency of the electric source. The parameter values are close to the case of Fig. 8c in the paper by Wilke et al. The Poincaré section thus obtained corresponds to a chaotic torus (Fig. 2). Note that a chaotic behavior structured around a torus is the type of behavior very often observed in glow discharge experiments, the gas being helium [1] or neon [7]. The Poincaré section obtained is not exactly similar to the one computed by Wilke and co-workers. This is not too relevant since there is a strong dependence on the initial conditions. Indeed, the set of Eqs. (11a)–(11c) defines a non-autonomous system. In such a case, there exists a continuum of attractors in the phase space [8]. In other words, changing the initial conditions is sufficient to switch from one attractor to another. Since the initial

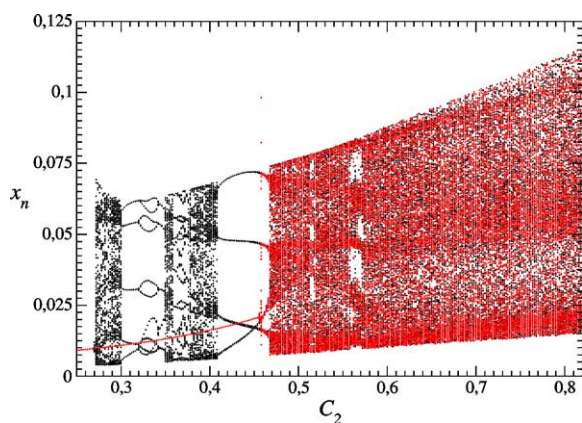


Fig. 3. Bifurcation diagram versus the parameter C_2 computed for the set of Eqs. (11a)–(11c) with parameters corresponding to Fig. 8c of Wilke’s paper with the exception of C_2 here equal to 0.294.

conditions are not provided in the work by Wilke et al., it is rather difficult to recover exactly the same attractor. The co-existence of many attractors in the phase space is easily exhibited by computing two bifurcation diagrams versus the parameter C_2 , one increasing and the other decreasing the parameter. It is easily observed that there is a certain range of the C_2 -parameter for which at least two different attractors coexist in the phase space (Fig. 3). The important point is therefore to recover a dynamics that is more or less structured around a torus as in the work by Wilke and co-workers.

Conversely, if we correct the sign of the diffusion term in Eq. (3), $-C_1$ becomes $+C_1$, and the dynamics is deeply changed. The behavior is no longer chaotic. The trajectory is ejected to infinity. This means that no stable physical behavior can be obtained and it is not possible to recover the mean value of dynamical variables as electron and excited atoms concentrations inside the discharge, the existence of a characteristic frequency for the previous variables, the oscillation of the discharge current in a linear regime for small perturbation amplitude of the voltage... [9–11]. Working with Eqs. (11a)–(11c) may eventually provide dynamics quite close to the experimental ones but cannot provide any explanation of the underlying physical processes. It is therefore necessary to improve the description of these processes to attempt a dynamics compatible with the observed dynamics.

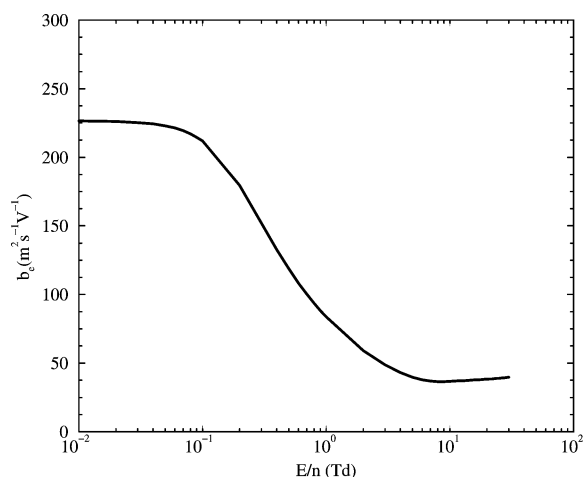


Fig. 4. Influence of the reduced electric field on the electron mobility calculated with Elendif under the conditions used by Wilke et al. [1].

3. An improved model

In order to explain the chaotic behavior in terms of chemistry, we modified Eqs. (11a)–(11c). In particular, we reconsidered the reaction rate for Penning ionization since this process implies non-linearities in the balance equations and, consequently, could be the relevant process for generating chaotic behaviors. Finally the propagation of electronic waves will be discussed.

3.1. The diffusion

Eq. (2) is used to calculate the ambipolar diffusion coefficient. The ion mobility b_p is constant and equal to $0.45 \text{ m}^2 \text{ s}^{-1} \text{ V}^{-1}$ for values of E/n less than 40 Td whereas it depends on the reduced electric field for higher values of E/n [12]. In this problem, the reduced electric field varies between 10 and 20 Td: therefore, we assumed that $b_p = 0.45 \text{ m}^2 \text{ s}^{-1} \text{ V}^{-1}$.

The electron mobility depends on E/n over an order of magnitude around 1 Td. We computed its evolution with the help of the Elendif solver allowing a temporal resolution of the Boltzmann equation [13]. Fig. 4 illustrates the results. For a reduced electric field varying between 10 and 20 Td, b_e is assumed to be constant and equal to $37.5 \text{ m}^2 \text{ s}^{-1} \text{ V}^{-1}$.

We have also calculated the mean electron energy $\langle e_e \rangle$ in order to obtain the parameter D_e with the

classical equation [14]:

$$D_e = \frac{2\langle e_e \rangle}{3m_e v_m}, \quad (15)$$

where m_e is the electron mass and v_m the momentum transfer collision frequency. v_m and $\langle e_e \rangle$ are calculated by Elendif. We obtained $v_m = 4.5 \times 10^9 \text{ s}^{-1}$ which does not depend on E/n and [15]:

$$\langle e_e \rangle = 2.92 \left(\frac{E}{n} \right)^{0.317}, \quad (16)$$

where $\langle e_e \rangle$ is in eV and E/n in Td. The ambipolar diffusion coefficient is thus found equal to:

$$D_{am} = 0.912 \left(\frac{E}{n} \right)^{0.317}. \quad (17)$$

According to the assumptions by Wilke et al., the diffusion of electrons and excited atoms (driven by the metastable one) are taken into account as in Eqs. (6) and (7) with $D_m = 0.045 \text{ m}^2 \text{ s}^{-1}$ [12].

3.2. The chemical reactions

The rate coefficients of chemical reactions are also reconsidered. The Elendif solver allows the calculation of the electron energy distribution function. It is thus possible to compute each rate coefficient for reaction under electron impact [15] starting from the most recent cross sections.

We used the cross section given by Shah et al. [16] for ionization of the fundamental state of He. We checked that the result is in good agreement with the calculation based on the cross sections obtained by Montague et al. [17] and Kim et al. [18]. Upon the interval considered for the reduced electric field, we thus obtained the relation:

$$z_{0\infty} = 1.8 \times 10^{-25} \left(\frac{E}{n} \right)^{5.6} \quad (18)$$

which is quite different from the one previously used. In addition, our value is systematically higher than the previous one as illustrated in Fig. 5. Despite a possible difference in the value of the cross section, the previous discrepancy probably results from the underestimation of the electrons in the *eedf* with an energy higher than the ionization limit. Indeed, this energy is 24.59 eV while the mean energy is lower than 8 eV for the electrons in the experimental conditions expressed

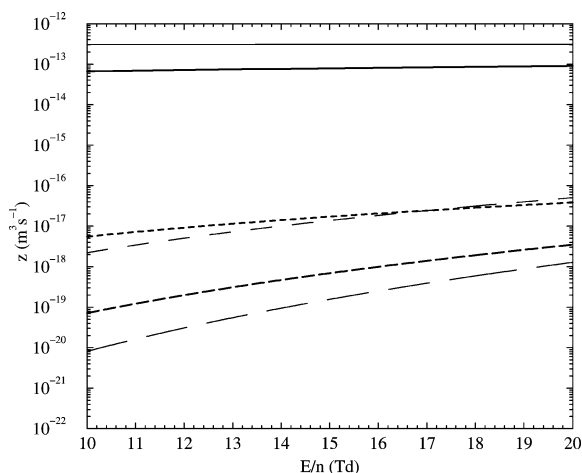


Fig. 5. Comparison between our rate coefficients (thick lines) and those used by Wilke et al. [1] (thin lines) for z_{me} (solid), z_{0a} (dashed) and $z_{0\infty}$ (long-dashed lines).

in Eq. (16). Consequently, this underestimation leads to an overestimation for excitation involving energies less than this mean energy. In the following, we shall point out this feature systematically. This problem is avoided in our case since the Boltzmann equation is solved by Elendif. We thus use these new results in the subsequent part of this Letter.

As far as we know, there is no recent data available for the calculation of the rate coefficient due to stepwise ionization of excited atoms under electron impact. We therefore adopted the form proposed by Wilke et al. for $z_{a\infty}$ even if, because of the previous problem mentioned for the *eedf*, the rate coefficient is probably lower.

Conversely, further information exists for the ionization of metastable atoms under electron impact. For the state He(2^3S) (19.82 eV from the ground), Dixon et al. [19] measured the cross section which is in good agreement with the calculation by Ivanovskii [20]. Raeker et al. [21] developed a model based on the R-matrix method and obtained values systematically lower than the experimental ones. The experimental results are thus considered for the calculation of $z_{me}(2^3S)$ and lead to:

$$z_{me}(2^3S) = 2.3 \times 10^{-14} \left(\frac{E}{n} \right)^{0.39}. \quad (19)$$

Another interest in the work by Raeker et al. is that they developed a calculation of the cross section

for the ionization of the metastable state He(2^1S) (20.62 eV from the ground) within the same model. Since, as far as we know, no experimental result is available, such a result may be a good basis for the determination of the rate coefficient $z_{me}(2^1\text{S})$. The cross section is systematically higher than for the He(2^3S) state as already calculated by Vriens [22] who showed that there exists a 3/2 ratio for the maximum of the cross section. By considering the ratio at each electron energy between the calculated cross section and the experimental one for the He(2^3S) state, by accounting for the shift of the maximum and the threshold, and by applying this ratio to the case of He(2^1S), we obtained after integration over the *eedf*:

$$z_{me}(2^1\text{S}) = 3.8 \times 10^{-14} \left(\frac{E}{n} \right)^{0.37}. \quad (20)$$

The global rate coefficient z_{me} is thus obtained by [23]:

$$z_{me} = \frac{z_{me}(2^1\text{S})n(2^1\text{S}) + z_{me}(2^3\text{S})n(2^3\text{S})}{n_a}.$$

Although the excitation energy difference between the metastable states is 0.8 eV, the mean electron energy is sufficiently high over the range for E/n in this problem to provide a local equilibrium between the two states. In this case, the density ratio is equal to the ratio of their statistical weights, and thus:

$$z_{me} = \frac{z_{me}(2^1\text{S}) + 3z_{me}(2^3\text{S})}{4}$$

which is interpolated under the form:

$$z_{me} = 2.4 \times 10^{-14} \left(\frac{E}{n} \right)^{0.44}. \quad (21)$$

This rate coefficient is lower than the one considered by Wilke et al. (cf. Fig. 5). Using a similar argument to that previously put forward for $z_{0\infty}$, the discrepancy between our results and those obtained by Wilke et al. could be explained by an overestimation by these authors for these electrons in the distribution function with an energy (in order of 4 eV) less than the mean value. This explanation does not hold when the cross section is involved.

We have also up-dated the value of the rate coefficient z_{0a} . Using the cross section of excitation under electron impact measured by Mason and Newell [24],

we obtained:

$$z_{0a} = 8.7 \times 10^{-21} \left(\frac{E}{n} \right)^{2.8}. \quad (22)$$

Although this rate coefficient does not take into account the excitation of levels other than the metastable ones, note that the previous value for z_{0a} is greater than the one considered by Wilke et al. over the most important part of the reduced electric field range. As previously discussed, the discrepancy may be explained in terms of estimation of *eedf*. Moreover, the calculations done with Elendif show that the mean energy of the electrons is significantly lower than the excitation energy of the metastable levels from the fundamental energy. The contribution of more excited levels to z_{0a} may therefore be neglected. We thus considered this value for z_{0a} in the following.

Fig. 5 shows the comparison between our rate coefficients and those used by Wilke et al. A significant discrepancy is observed: a ratio of 10 can be observed for specific conditions. Chemistry induces nonlinearities in the set of equations as already shown by Eqs. (11a)–(11c). Consequently, the value of the rate coefficients can influence significantly the asymptotic behavior. Thus, these new values are used in Section 3.4.

Finally, we discuss the rate coefficient z_a for Penning ionization. Much work has been devoted to its determination. For ambient temperature, Johnson and Gerardo [25] measured: $z_a = 4.5 \times 10^{-15} \text{ m}^3 \text{ s}^{-1}$. This value is also used by Shirafuji et al. [26]. Since Johnson and Gerardo determined this rate coefficient from the measurement of the density of the metastable atoms, the dissociative recombination of He_2^+ may be the origin of an overestimation of z_a .

Otherwise, Lee et al. [27] used $z_a = 6.2 \times 10^{-16} \text{ m}^3 \text{ s}^{-1}$ which is in very good agreement with the value determined by Kristian [28] ($z_a = 7 \times 10^{-16} \text{ m}^3 \text{ s}^{-1}$). Note that these values are lower than the previous ones. Kolokolov and Blagoev [29] have studied the global rate coefficient for simultaneous Penning effect and associative ionization for helium for which the metastable state involved is known. The global rate coefficient is about $10^{-14} \text{ m}^3 \text{ s}^{-1}$ which is much higher than the previous values for z_a . The probability for associative ionization being significantly lower than that for Penning ionization [30], the order of magnitude for z_a may be higher than 10^{-16} – $10^{-15} \text{ m}^3 \text{ s}^{-1}$.

Table 3

Rate coefficient z_a for Penning ionization. The last column gives the non-dimensional values of z_a denoted α_P

Reference	Year	z_a ($\text{m}^3 \text{s}^{-1}$)	$\alpha_P = 10^{-10} n z_a$
Johnson et al. [25]	1973	4.5×10^{-15}	0.0261
Kolokolov et al. [29]	1993	10^{-14}	0.0579
Kristian. [28]	1996	7×10^{-16}	0.0041
Lee et al. [27]	1997	6.2×10^{-16}	0.0036
Muller et al. [30]	1991	1.79×10^{-15}	0.0104
Neynaber et al. [31]	1978	1.96×10^{-15}	0.0114

For low energies, there is little recent information about the Penning ionization cross section. Experimentally, over the interval $10 \leq E \leq 100$ MeV, Neynaber et al. [31] have determined the evolution of the total cross section for Penning and associative ionizations towards the kinetic energy E of the collision partners. As the associative ionization amounts to 10% of the total ionization, for the Penning effect these authors deduced the cross section:

$$\sigma_P(E) = \sigma_0 \left(\frac{E_0}{E} \right)^\alpha \quad (23)$$

with $\sigma_0 = 112 \times 10^{-20} \text{ m}^2$, $E_0 = 33 \text{ MeV}$ and $\alpha = 0.38$. We calculated that for 300 K this cross section leads to $z_a = 1.96 \times 10^{-15} \text{ m}^3 \text{ s}^{-1}$. More recently, Muller et al. [30] experimentally and theoretically investigated this cross section. They proposed the same equation as Eq. (23) but with $\sigma_0 = 103 \times 10^{-20} \text{ m}^2$, $E_0 = 33 \text{ MeV}$ and $\alpha = 0.28$. With these conditions, we estimated that z_a should instead be equal to $1.79 \times 10^{-15} \text{ m}^3 \text{ s}^{-1}$ for 300 K.

Table 3 sums up the z_a values available in the literature. No one value seems to be preferred. The rate coefficient for Penning ionization is thus: $z_a = (5 \pm 4) \times 10^{-15} \text{ m}^3 \text{ s}^{-1}$.

3.3. The propagation of electronic waves

The ionization waves are mainly characterized by an oscillation of the structure of the *eedf* as clearly pointed out by Rayment and Twiddy [3]. Their experiment was done with neon but all the following characteristics may be extended to helium as well as the other noble gases. Using a fast Langmuir probe, they showed with time-resolved measurements that these waves are related to the crossing of areas where the electric field is very high and have an influence

upon the *eedf* without a direct relation with the external field applied. The latter distribution is double-peaked. The corresponding electrons are in fact those accelerated by the strong reduced electric field (80 Td in order of magnitude in their case) and produce secondary electrons with less energy by inelastic collisions. The distribution is also unsteady. When the field decreases, the highest peak moves toward higher energy and vanishes. It is important to note that these results are related to different conditions for the discharge than in our case: the current (330 mA) is much greater and the pressure lower (0.32 Torr) in a gas (neon) for which the ionization limit (21.56 eV) is lower. Thus, the *eedf* is closer in our case to a Maxwellian one as shown by Elendif: it is therefore not double-peaked, quasi-steady and E/n is much lower. But the general behavior is the same: the waves are characterized by moving areas where E/n is high and not equal to the external electric field leading to the oscillation of the collected light flux. The distribution of E/n is hence spatially periodic.

Using a Langmuir probe different from that of Rayment and Twiddy, Van Den Berge and Vermeulen [36] pointed out the periodic behavior in a given location of the mean electron energy $\langle e_e \rangle$. This parameter is related to the reduced electric field by Eq. (16). Therefore E/n behaves identically. As a result, the characteristics of the total flux intensity mentioned in Section 1 are not only due to the oscillation of population densities for the excited atoms but also to the specific behavior for E/n .

The main consequence is that uniformity of the reduced electric field is impossible: electroneutrality cannot therefore be satisfied. Electrons and ions have to be separately balanced. This is an additional reason to modify the model by Wilke et al.

In fact, the electron and ion densities are thus related to the gradient of the quasi-static electric field by Poisson's equation:

$$\frac{\partial E}{\partial x} = \frac{(n_i - n_e)e}{\epsilon_0}, \quad (24)$$

where e is the absolute value of the electron charge and ϵ_0 the permittivity of the vacuum. Consequently, electrons and ions axially diffuse separately. For electrons, the diffusion flux density accounts for the contribution of the drift due to the electric field and the thermal dif-

fusion:

$$I_e = -n_e b_e E - D_e \frac{\partial n_e}{\partial x} \quad (25)$$

while the diffusion flux density related to the ions is reduced to the influence of E , the diffusion coefficient being negligibly small:

$$I_i = +n_i b_p E. \quad (26)$$

Very recently Golubovskii et al. developed a kinetic model based upon the Boltzmann equation written under a form suitable for weak anisotropy to explain the propagation of the ionization waves in such discharges [32,33]. With our approach using Elendif, such assumptions do not necessarily improve the validity of the results. Starting from an arbitrary spatially modulated profile, they showed that a phase shift appears between the maximum of the ionization rate and that of the electron density. Such a shift stimulates the propagation of the waves as a result of non-local effects. By non-local effects, we mean that the local density for electrons as well as all integrals of the *eedf* result not only from the local value of the reduced electric field but also from the value of its gradient. Eqs (25) and (26) show that such a relationship is ensured, the balance equation for ions and electrons (see Eqs. (28) and (30)) accounting for the gradient of their flux density.

The macroscopic scales of the ionization waves are significantly larger than the microscopic scales (Debye lengths). Nevertheless, the departure from quasi-neutrality as previously claimed must be addressed. Indeed, Eq. (24) allows to justify that quasi-neutrality is not valid.

The common value for the electron density measured in such a discharge is $n_e \simeq 10^{15} - 10^{16} \text{ m}^{-3}$. Assuming a departure from neutrality equal to 0.1% only, Eq. (24) leads to:

$$\frac{\partial E}{\partial x} \simeq (2-20) \times 10^4 \text{ V m}^{-2} \quad (27)$$

that is the order of magnitude calculated by Golubovskii et al. [34,35] in the vicinity of the ionization wave front in a neon discharge. On the other hand, Van Den Berge and Vermeulen measured the mean electron energy in moving striations with Langmuir probes [36]. Thus, when a wave front crosses the probe with the speed $v = 150 \text{ m s}^{-1}$, they obtained:

$$\frac{\partial \langle e_e \rangle}{\partial t} \simeq 4 \times 10^4 \text{ eV s}^{-1}$$

and $\langle e_e \rangle \simeq 9 \text{ eV}$. Calculating with Elendif the following relationship between $\langle e_e \rangle$ and E/n for neon:

$$\langle e_e \rangle = 4.90 \left(\frac{E}{n} \right)^{0.209}$$

and assuming that the waves are neither excited nor damped during their propagation with constant velocity, we thus obtain the value for the gradient of the electric field:

$$\frac{\partial E}{\partial x} \simeq 6.5 \times 10^4 \text{ V m}^{-2}$$

in good agreement with Eq. (27). Consequently, even small deviations from electroneutrality can explain the gradient of the electric field. Our aim in elaborating this new model is to identify the main processes responsible for the behaviors described in Sections 1 and 2 where the waves could play a very important role: the assumption of electroneutrality has to be abandoned.

The discharge region where it is well known that electroneutrality is not fulfilled is near the cathode. For helium, the previous orders of magnitude for $\frac{\partial E}{\partial x}$, $\langle e_e \rangle$, E/n and n_e have been measured by Sirghi et al. [37]. It seems that the electric gradient occurring in an ionization wave is similar as gradient observed in the cathode region. Under the conditions here considered, quasi-neutrality is definitely not fulfilled.

Finally, we assume that the diffusion toward the wall is purely ambipolar. The approach by Wilke et al. is thus used.

3.4. The new set of equations

According to the previous discussion:

- Eq. (6) should be rewritten under the form:

$$\begin{aligned} \frac{\partial n_e}{\partial t} + \frac{\partial}{\partial x} \left(-D_e \frac{\partial n_e}{\partial x} \right) + \frac{\partial}{\partial x} (-n_e b_e E) \\ + \frac{\lambda_1^2 D_{am} n_e}{r_0^2} - n n_e z_{0\infty} - 1.45 n_a n_e z_{a\infty} \\ - 1.45 n_a^2 z_a = 0; \end{aligned} \quad (28)$$

- Eq. (7) as:

$$\begin{aligned} \frac{\partial n_a}{\partial t} + \frac{\lambda_1^2 D_{mna}}{r_0^2} + 2.9 n_a^2 z_a + 1.45 n_e n_a z_{me} \\ + 1.45 n_e n_a z_{a\infty} - n n_e z_{0a} = 0; \end{aligned} \quad (29)$$

- and the balance equation for ions as:

$$\frac{\partial n_i}{\partial t} + \frac{\partial}{\partial x}(n_i b_p E) + \frac{\lambda_1^2 D_{am} n_i}{r_0^2} - n n_e z_{0\infty} - 1.45 n_a n_e z_{a\infty} - 1.45 n_a^2 z_a = 0. \quad (30)$$

With the variables defined by Eq. (10) and:

$$W = 10^6 \frac{n_i}{n}, \quad \bar{x} = \frac{x}{l_0} \quad (31)$$

we obtain the new system of equations:

$$\begin{aligned} \frac{\partial X}{\partial \tau} - 4.53 \times 10^{-2} \frac{\partial}{\partial \bar{x}} \left[\left(\frac{E}{n} \right)^{0.317} \frac{\partial X}{\partial \bar{x}} \right] \\ - 0.53 \frac{\partial}{\partial \bar{x}} \left[\left(\frac{E}{n} \right) X \right] + 5.26 \left(\frac{E}{n} \right)^{0.317} X \\ - 1.044 \times 10^{-6} \left(\frac{E}{n} \right)^{5.6} X - 0.227 \left(\frac{E}{n} \right)^{0.65} XY \\ - 1.45 \alpha_P Y^2 = 0, \end{aligned} \quad (32a)$$

$$\begin{aligned} \frac{\partial Y}{\partial \tau} + 0.259 Y + 2.9 \alpha_P Y^2 + \left[0.202 \left(\frac{E}{n} \right)^{0.44} \right. \\ \left. + 0.227 \left(\frac{E}{n} \right)^{0.65} \right] XY - 0.0505 \left(\frac{E}{n} \right)^{2.8} X = 0, \end{aligned} \quad (32b)$$

$$\begin{aligned} \frac{\partial W}{\partial \tau} + 6.37 \times 10^{-3} \frac{\partial}{\partial \bar{x}} \left[\left(\frac{E}{n} \right) W \right] \\ + 5.26 \left(\frac{E}{n} \right)^{0.317} W - 1.044 \times 10^{-6} \left(\frac{E}{n} \right)^{5.6} X \\ - 0.227 \left(\frac{E}{n} \right)^{0.65} XY - 1.45 \alpha_P Y^2 = 0, \end{aligned} \quad (32c)$$

$$\frac{\partial(E/n)}{\partial \bar{x}} = 7.42 \times 10^6 (W - X), \quad (32d)$$

where E/n is expressed in units of Td.

3.5. The boundary conditions

For several authors, notably Emel us and Daly [38] and Loeb [39], it seems that the moving striations may originate when the ions oscillate in a potential minimum near the cathode. In this region, our model is not valid: indeed, the ions are highly accelerated by the electric field in the sheath, heating by charge

transfer the neutral particles which in turn heat the electrode. Moreover, they bombard the latter and produce secondary electrons: the behavior is thus completely different from that in the positive column of the discharge for which the model of this Letter has been elaborated.

The boundary conditions considered are consequently related to the positive column itself and make no distinction between the electrodes. If the source of striations is an oscillation of the ions, we may be able to reveal it by a periodic disturbance of the external voltage.

The currents calculated at each side of the discharge:

$$i = \pi r_0^2 e (I_i - I_e)$$

are therefore identical. We have:

$$\begin{aligned} i = 5.41 \times 10^{-4} \left[\left(\frac{E}{n} \right)^{0.317} \frac{\partial X}{\partial \bar{x}} + 11.7 \left(\frac{E}{n} \right) X \right. \\ \left. + 0.141 \left(\frac{E}{n} \right) W \right]_{\bar{x}=0} \\ = 5.41 \times 10^{-4} \left[\left(\frac{E}{n} \right)^{0.317} \frac{\partial X}{\partial \bar{x}} + 11.7 \left(\frac{E}{n} \right) X \right. \\ \left. + 0.141 \left(\frac{E}{n} \right) W \right]_{\bar{x}=1}, \end{aligned} \quad (33)$$

where E/n is expressed in units of Td.

Moreover, the balance equation for the external circuit leads to:

$$U_-(1 + m \cos \Omega \tau) = 23.8 \int_0^1 \left(\frac{E}{n} \right) d\bar{x} + Ri. \quad (34)$$

4. Conclusion

We put forward the model elaborated by Wilke et al. to explain the behavior of a helium glow discharge for particular conditions where prechaotic and chaotic regimes are obvious. We show that this model had to be improved since some physical principles were not satisfied. Correcting some of them induced, for example, the change of the sign of the electron diffusion term; the first model thus became inoperant to properly describe the underlying dynamics.

We therefore present an improved model which is mainly based upon the assumption of a separate motion for charged particles and uses an up-dated set of rate coefficients calculated with the help of a solver to treat the Boltzmann equation. This directly results from the non-uniform electric field characterizing the moving striations inside the discharge; it is likely that these striations cause the chaotic regimes. This new model is no longer constituted with ordinary differential equations but with partial differential equations which are much more tricky to integrate. The numerical investigation of the dynamics generated by this new model is therefore postponed for future work.

Acknowledgements

C.L. wishes to thank C. Wilke and A. Dinklage for motivating his interest in glow discharge experiments. With A.B. they thank also G. Bonhomme for helpful discussions about glow discharge dynamics. The authors wish to thank also D. Moscato for improving English.

References

- [1] C. Wilke, R.W. Leven, H. Deutsch, Phys. Lett. A 136 (3) (1989) 114.
- [2] H.S. Robertson, Phys. Rev. 105 (2) (1957) 368.
- [3] S.W. Rayment, N.D. Twiddy, J. Phys. D 2 (2) (1969) 1747.
- [4] J.A. Walkenstein, W.B. Pardo, M. Monti, R.E. O'Meara, T.N. Buch, E. Rosa Jr., Phys. Lett. A 261 (1999) 183.
- [5] B.P. Koch, N. Goepf, B. Bruhn, Phys. Rev. E 56 (2) (1997) 2118.
- [6] R. Deloche, P. Monchicourt, M. Cheret, F. Lambert, Phys. Rev. A 13 (3) (1979) 1140.
- [7] C. Letellier, A. Dinklage, H. El-Naggar, C. Wilke, G. Bonhomme, Phys. Rev. E 63 (2001) 042702.
- [8] O. Ménard, C. Letellier, J. Maquet, L. Le Sceller, G. Gouesbet, Int. J. Bifur. Chaos 10 (7) (2000) 1759.
- [9] H. Amemiya, J. Phys. D: Appl. Phys. 17 (1984) 2387.
- [10] H.F. Wellenstein, W.W. Robertson, J. Appl. Phys.: Appl. Phys. 43 (1972) 4823.
- [11] A.T. Jackson, J.R.M. Coulter, J. Phys. A: Gen. Phys. 3 (1970) 559.
- [12] J.B. Hasted, Physics of Atomic Collisions, Butterworths, London, 1964.
- [13] W.L. Morgan, B.M. Penetrante, Comput. Phys. Commun. 58 (1990) 127.
- [14] L.G.H. Huxley, Atomic and Molecular Processes, Academic Press, New York, 1962, Chapter: The motions of slow electrons in gases, p. 335.
- [15] A. Bultel, A. Bourdon, C. Letellier, Modélisation d'une décharge dans l'hélium, UMR CNRS 6614 CORIA, 2002.
- [16] M.B. Shah, D.S. Elliott, P. McCallion, H.B. Gilbody, J. Phys. B: At. Mol. Opt. Phys. 21 (1988) 2751.
- [17] R.G. Montague, M.F.A. Harrison, A.C.H. Smith, J. Phys. B: At. Mol. Opt. Phys. 17 (1984) 3295.
- [18] Y.-K. Kim, W.R. Johnson, M.E. Rudd, Phys. Rev. A 61 (2000) 034702.
- [19] A.J. Dixon, M.F.A. Harrison, A.C.H. Smith, J. Phys. B: At. Mol. Phys. 9 (15) (1976) 2617.
- [20] A.L. Ivanovskii, Zh. Eksp. Teor. Fiz. 104 (1993) 3928.
- [21] A. Raeker, K. Bartschat, R.H.G. Reid, J. Phys. B: At. Mol. Opt. Phys. 27 (1994) 3129.
- [22] L. Vriens, Phys. Lett. 8 (4) (1964) 260.
- [23] A. Bultel, P. Vervisch, J. Phys. B: At. Mol. Opt. Phys. 35 (2002) 111.
- [24] N.J. Mason, W.R. Newell, J. Phys. B: At. Mol. Phys. 20 (1987) 1357.
- [25] A.W. Johnson, J.B. Gerardo, Phys. Rev. A 7 (3) (1973) 925.
- [26] T. Shirafuji, K. Tachibana, Y. Matsui, Jpn. J. Appl. Phys. 34 (1995) 4239.
- [27] Y.T. Lee, M.A. Lieberman, J. Lichtenberg, F. Bose, H. Baltes, R. Patrick, J. Vac. Sci. Technol. A 15 (1) (1997) 113.
- [28] V.I. Kristian, Teplofiz. Vys. Temp. 34 (2) (1996) 197.
- [29] N.B. Kolokolov, A.B. Blagoev, Phys. Usp. 36 (3) (1993) 152.
- [30] M.W. Muller, A. Merz, M.-W. Ruf, H. Hotop, W. Meyer, M. Movre, Z. Phys. D: At. Mol. Clusters 21 (1991) 89.
- [31] R.H. Neynaber, G.D. Magnuson, S.Y. Tang, J. Chem. Phys. 68 (1978) 5112.
- [32] Y.B. Golubovskii, V.A. Maiorov, I.A. Porokhova, J. Behnke, J. Phys. D: Appl. Phys. 32 (1999) 1391.
- [33] Y.B. Golubovskii, V.A. Maiorov, V.O. Nekutchev, J. Behnke, J.F. Behnke, Phys. Rev. E 63 (2001) 036409.
- [34] Y.B. Golubovskii, V.A. Maiorov, R.V. Kozakov, S. Solyman, G. Stockhausen, C. Wilke, J. Phys. D: Appl. Phys. 34 (2001) 1963.
- [35] Y.B. Golubovskii, R.V. Kozakov, V.A. Maiorov, J. Behnke, J.F. Behnke, Phys. Rev. E 2 (2) (2001) 1963.
- [36] G. Van Den Berge, D. Vermeulen, J. Phys. E: Sci. Instrum. 9 (1976) 819.
- [37] L. Sirghi, K. Ohe, G. Popa, J. Phys. D: Appl. Phys. 31 (1998) 551.
- [38] K.G. Emeléus, N.R. Daly, Proc. Phys. Soc. London, Sect. B 433 (1956) 114.
- [39] L.B. Loeb, Phys. Rev. 76 (2) (1949) 255.